ChemComm

COMMUNICATION

View Article Online
View Journal | View Issue

Cite this: *Chem. Commun.*, 2022, **58**, 6853

Received 28th February 2022,
Accepted 17th May 2022

DOI: 10.1039/d2cc01229d

rsc.li/chemcomm

Tuning the photophysical properties of luminescent lanthanide complexes through regioselective antenna fluorination†

Daniel Kocsi, Andreas Orthaber and K. Eszter Borbas *

Carbostyrils monofluorinated in the 3, 5, or 6 positions were synthesised from olefinic precursors *via* a photochemical isomerisation-cyclisation route, and incorporated into octadentate cyclen triacetate ligands that formed luminescent complexes with Tb(III) and Eu(III). The photophysical properties of the emitters were strongly dependent on the position of the fluorination.

The luminescence of the trivalent lanthanide (Ln) ions is applied in diverse biological and industrial settings ranging from the monitoring of the components of living cells to the thermometric analysis of materials.[1,2] Ln(III) luminescence is often sensitised by a light-harvesting antenna to avoid the need for direct excitation of the Laporte-forbidden 4f–4f transitions.[3] Optimisation of energy transfer (EnT) to the Ln(III) and elimination of processes that quench the antenna and Ln(III) excited states are essential for bright emitters.

Photoinduced electron transfer (PeT) from the excited antenna to Ln(III) is feasible for several Lns,[4,5] and for Eu(III) emission it can be an effective luminescence quenching process.[6] PeT is suppressed when the antenna is less reducing. Antenna substitution with electron-withdrawing groups (*e.g.* with CF_3, Fig. 1)[4,5] or protonation[7,8] can increase the Eu(III) luminescence quantum yield, but may have unintended consequences on the antenna excited state energies.[5,9,10] Ln sensitisation commonly takes place *via* the antenna singlet (S_1) and triplet excited states (T_1). Even subtle changes to the antenna may alter the S_1 and T_1 energies and EnT. In the previous examples both antenna trifluoromethylation[4,5] and protonation proved detrimental to Tb(III) emission.[8]

Here, we have prepared three monofluorinated 7-aminocarbostyril regioisomers. Electronegative fluorine was expected to decrease PeT by making the antenna less reducing, a strategy that complements the use of C–F bonds to replace the more efficiently quenching C–H oscillators.[11] Fluorination has additional potential benefits. Fluorine is a hydrogen isostere conferring metabolic stability, H-bond acceptor ability, and altered lipophilicity on pharmaceuticals.[12] Diagnostic applications of fluorinated probes include multimodal[13] and responsive[14] systems. ^{19}F-MRI is a promising low-background technique,[15] and ^{18}F is an attractive PET label.[16,17]

Fluorinated carbostyrils were incorporated into do3a (1,4,7,10-tetraazacyclododecane-1,4,7-triacetate)-based octadentate ligands to enable comparison with previously reported structures.[4,5] The Eu(III), Tb(III), and Gd(III) chelates of the ligands were characterised using ^{1}H NMR spectroscopy, cyclic voltammetry, and UV-vis absorption and steady-state and time-resolved emission spectroscopies. Our results show fluorination meaningfully impacts the antenna and Ln(III) photophysical properties, and substitution at a remote antenna position could even influence the excited state behaviour of the Ln(III).

Fluorinated antennae were synthesised as shown in Scheme 1 and Schemes S1–S6 (ESI†). The procedures were

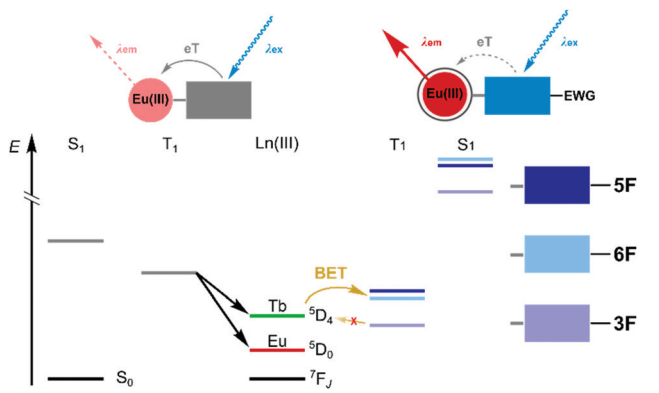

Fig. 1 Decreased PeT quenching of Eu(III) luminescence through antenna substitution with electron-withdrawing group(s) (EWG), and its effects on the S_1 and T_1 energies.

Department of Chemistry, Ångström Laboratory, Uppsala University, Lägerhyddsvägen 1, 75120, Uppsala, Sweden. E-mail: eszter.borbas@kemi.uu.se

† Electronic supplementary information (ESI) available: Synthesis, characterisation, and NMR spectra of all new compounds, additional crystallographic, photophysical, and electrochemical characterisation. CCDC 2155036–2155038. For ESI and crystallographic data in CIF or other electronic format see DOI: https://doi.org/10.1039/d2cc01229d

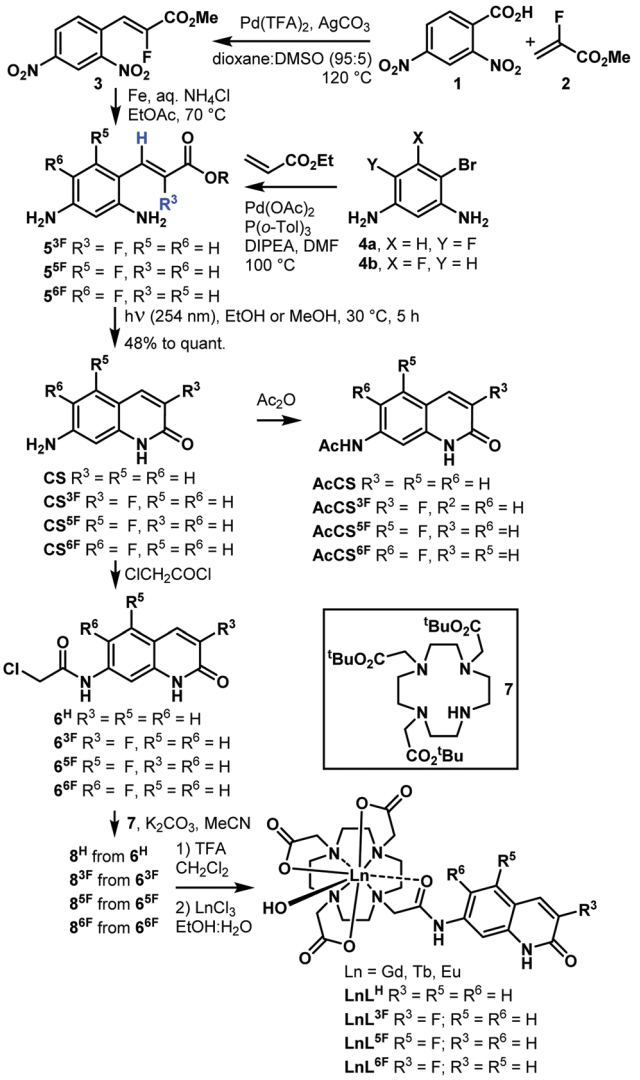

Scheme 1 Preparation of **CS**$^{\mathbf{F}}$, **AcCS**, **AcCS**$^{\mathbf{F}}$, and **LnL**$^{\mathbf{F}}$.

robust, scalable (*e.g.* 466 mg of **CS**$^{\mathbf{6F}}$ was obtained in one experiment), and reproducible. Olefins **5**$^{\mathbf{F}}$ were prepared from commercially available starting materials as the *Z* isomers with excellent selectivity due to the steric clash between the ester group and the aromatic ring.[18] The stereochemical assignment was based on the $^{3}J_{HF}$ = 33–38 Hz and $^{3}J_{HH}$ = 15–16 Hz coupling constants. The key photochemical olefin isomerisation-cyclisation was carried out by irradiating a 100 mM solution of **5** in MeOH or EtOH with 254 nm-UV light, giving **CS**$^{\mathbf{3F}}$, **CS**$^{\mathbf{5F}}$, and **CS**$^{\mathbf{6F}}$ in good to excellent yield. Regioisomer identities were confirmed by 1D and 2D NMR spectroscopy and single-crystal X-ray crystallography (Fig. S1–S6 and Tables S1–S3, ESI†). The analogous **CS**$^{\mathbf{4F}}$ could not be accessed *via* similar routes due to the instability of the intermediates (Schemes S3–S5, ESI†). **CS**/**CS**$^{\mathbf{F}}$ was acetylated with Ac_2O or chloroacetyl chloride to yield reference compounds **AcCS**/**AcCS**$^{\mathbf{F}}$, or the reactive antennae **6**, respectively. **6** were incorporated into **LnL** (Ln = Gd, Eu, Tb) using procedures previously developed for similar compounds. Synthetic details, compound characterisations, and the attempted syntheses of **CS**$^{\mathbf{4F}}$ are given in the ESI.† Analytical data were fully consistent with the assigned structures.

Solution structures of **EuL**$^{\mathbf{F}}$ were studied by paramagnetic ^{1}H and ^{19}F NMR spectroscopy. In CD_3OD at r.t. the ^{1}H NMR spectra of **EuL**$^{\mathbf{3F}}$, **EuL**$^{\mathbf{5F}}$, **EuL**$^{\mathbf{6F}}$, and **EuL**$^{\mathbf{H}}$, were similar (Fig. S7–S10, ESI†). The major isomer had square antiprismatic geometry (4 peaks at >32 ppm). Trace amounts of the twisted square antiprismatic isomer were also present (signals at 12–16 ppm). ^{19}F NMR spectra supported this interpretation, showing a single peak at −133.8, −118.8, and −134.1 ppm for **EuL**$^{\mathbf{3F}}$, **EuL**$^{\mathbf{5F}}$, and **EuL**$^{\mathbf{6F}}$, respectively (Fig. S11–S13, ESI†). These data are consistent with the ligands imposing similar geometries on the Ln(III) ions in solution in the ground state, and is similar to what has been observed for other do3a-complexes carrying carbostyril antennae.[6] This was expected as fluorine is small, and the fluorination sites are quite distant from the Ln(III).

The photophysical properties of **CS** and **CS**$^{\mathbf{F}}$ were recorded in acetonitrile due to their low aqueous solubility. The lowest-energy bands in the absorption spectra were assigned to π–π* transitions, and were located at 320–360 nm with λ_{max} = 335, 332, and 339 nm for **CS**$^{\mathbf{3F}}$, **CS**$^{\mathbf{5F}}$, and **CS**$^{\mathbf{6F}}$, respectively (Fig. S18–S22, ESI†), non-fluorinated **CS** had λ_{max} = 337 nm. **CS**, **CS**$^{\mathbf{3F}}$, **CS**$^{\mathbf{5F}}$, and **CS**$^{\mathbf{6F}}$ excitation at λ_{max} resulted in fluorescence emission maxima at λ_{em} = 384, 400, 387, and 382 nm, respectively (Table 1 and Fig. S23–S27, ESI†). **CS**$^{\mathbf{3F}}$ had the highest fluorescence quantum yield, Φ_L = 56%. Fluorination in the 5-position had minimal effect on Φ_L compared to **CS** (Φ_L = 25 and 27%, respectively), while substitution in the 6-position lowered Φ_L to 10%. **CS**$^{\mathbf{F}}$ fluorescence lifetimes (τ_{fl}) mirrored the observations made for Φ_L (Table 1). **CS**$^{\mathbf{3F}}$ had the longest τ_{fl} (2.84 ns), and **CS**$^{\mathbf{6F}}$ the shortest, τ_{fl} = 0.41 ns. **CS** and **CS**$^{\mathbf{5F}}$ had very similar τ_{fl}, 1.15 and 1.09 ns, respectively (Table S5 and Fig. S49–S56, ESI†).

LnL absorption spectra were collected in aqueous solutions (0.01 M PIPES buffer, pH = 6.5). Absorption maxima were blue-shifted relative to the corresponding **CS** with λ_{max} = 325, 327, 337, and 330 nm for **LnL**$^{\mathbf{3F}}$, **LnL**$^{\mathbf{5F}}$, **LnL**$^{\mathbf{6F}}$, and **LnL**$^{\mathbf{H}}$, respectively (Fig. 2 and Fig. S28–S32, ESI†).

Gd(III) excited states are too high to accept energy from the antennae, therefore, **GdL** are useful for determining the

Table 1 Photophysical properties of **CS**, **CS**$^{\mathbf{F}}$,[a] and **GdL**$^{\mathbf{F}}$ [b]

	λ_{max} (nm)	λ_{em}[c] (nm)	S_1 (cm^{-1})	T_1[d] (cm^{-1})	Φ_L[e] (%)	τ_{fl} (ns)
CS	337	384	—	—	27	1.15 (5)
CS$^{\mathbf{3F}}$	335	400	—	—	56	2.84 (6)
CS$^{\mathbf{5F}}$	332	387	—	—	25	1.09 (2)
CS$^{\mathbf{6F}}$	339	382	—	—	10	0.41 (6)
GdL$^{\mathbf{H}}$	330	369	28 700	22 500	7.6	0.34 (3)
GdL$^{\mathbf{3F}}$	325	364	29 200	22 100	13	0.60 (5)
GdL$^{\mathbf{5F}}$	327	367	28 900	22 400	6.1	0.44 (8)
GdL$^{\mathbf{6F}}$	337	380	28 100	22 300	5.9	0.36 (4)

[a] In acetonitrile at 10 μM concentration. [b] In aqueous PIPES buffer (10 mM), pH 6.5, at 10 μM complex concentrations. [c] λ_{ex} = 332 nm (**CS**$^{\mathbf{3F}}$), 331 nm (**CS**$^{\mathbf{5F}}$), 338 nm (**CS**$^{\mathbf{6F}}$), 335 nm (**GdL**$^{\mathbf{6F}}$), 327 nm (**GdL**$^{\mathbf{5F}}$), 325 nm (**GdL**$^{\mathbf{3F}}$). [d] Calculated from the 0–0 transitions of the Gd-complexes recorded at 77 K. [e] Relative to quinine sulfate (Φ = 0.59) in H_2SO_4 (0.05 M).[23]

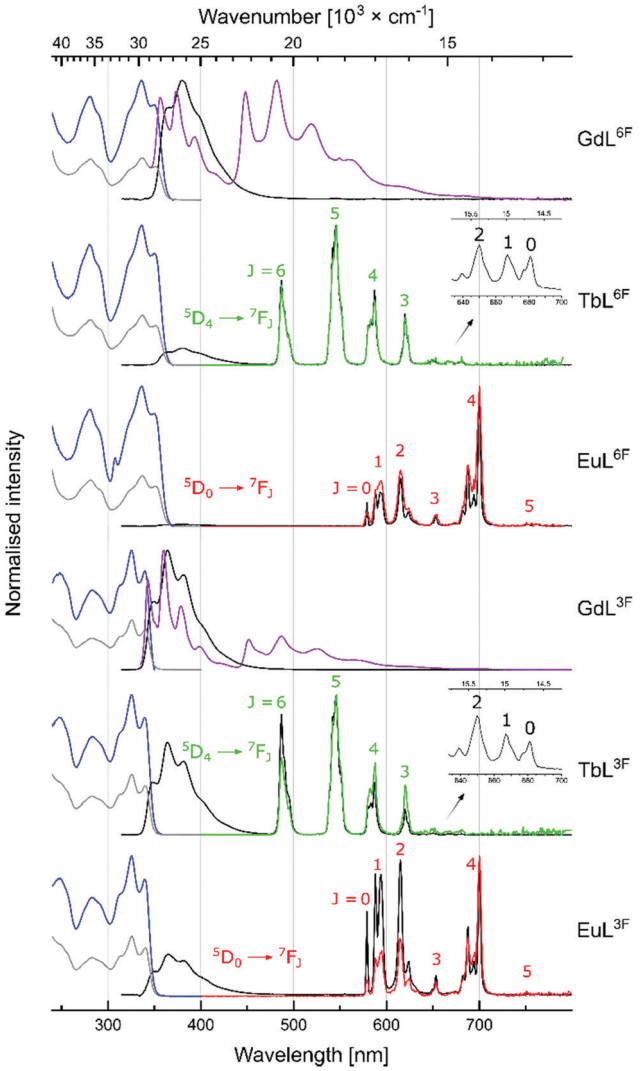

Fig. 2 Normalised absorption (grey, 298 K), excitation [blue, λ_{em} = 380 nm (**GdL^{6F}**), λ_{em} = 364 nm (**GdL^{3F}**), λ_{em} = 546 nm (Tb), λ_{em} = 615 nm (Eu), 298 K], steady-state emission at 298 K [black, λ_{ex} = 335 nm (**LnL^{6F}**), λ_{ex} = 325 nm (**LnL^{3F}**)], steady-state emission at 77 K [purple, λ_{ex} = 335 nm (**LnL^{6F}**), λ_{ex} = 325 nm (**LnL^{3F}**)] and time-resolved emission [green (Tb), red (Eu), λ_{ex} = 335 nm (**LnL^{6F}**), λ_{ex} = 325 nm (**LnL^{3F}**), 298 K] spectra of **LnL^{F}**.

antenna photophysical properties in **LnL** without interference from photo- or redox-active Ln(III). Carbostyril excitation in **GdL** returned antenna fluorescence that was blue-shifted and less intense than that of the corresponding 7-aminocarbostyril (Fig. S33–S36, ESI†). Φ_L was largest for **GdL^{3F}** (13%) and smallest for **GdL^{6F}** (5.9%), with Φ_L(**GdL^{5F}**) = 6.1% and Φ_L(**GdL^{H}**) = 7.6% in between. Steady state emission spectra were recorded at 77 K to determine the antenna T_1 (Fig. S45–S48, ESI†). Notably, fluorination in all three investigated positions lowered the antenna T_1 from 22 500 cm^{-1} in **GdL^{H}**. **GdL^{3F}** had the lowest energy T_1 (22 100 cm^{-1}), and **GdL^{5F}** had the highest, at only 300 cm^{-1} higher energy. These are small but impactful differences. The $^5D_4$ emitting level of Tb(III) is located at 20 400 cm^{-1}, and the antenna T_1 must be at least ~2000 cm^{-1} higher energy to avoid thermal back energy transfer (BET). Thus, **TbL^{3F}** and possibly even **TbL^{6F}** (but likely not **TbL^{5F}**) may be susceptible to BET. Tb(III) complexes that undergo BET are oxygen sensitive, and are useful for O_2-sensing and cytotoxic singlet oxygen generation.[19,20] T_1 are ~5000 cm^{-1} higher than the emissive $^5D_0$ level of Eu(III), which is suitable for Eu(III) sensitization.[21] T_1 in **LnL^{F}** are closer to the accepting $^5D_2$ Eu(III) level (21 500 cm^{-1}) than in **LnL^{H}**, which may result in better energy transfer in the fluorinated complexes.[21,22]

Excitation of **TbL** and **EuL** at λ_{max} yielded green and red Ln(III) luminescence, respectively (Fig. 2 and Fig. S37–S44, ESI,† Table 2), with residual antenna fluorescence. **TbL** had slightly lower Φ_L than the analogous **GdL** likely due to some antenna S_1-mediated EnT to Tb(III).[6] **EuL** had drastically diminished Φ_L, which may be due to a combination of EnT from S_1, and depopulation of S_1 by PeT. **AcCS^{F}** oxidation potentials (E_{ox}) were found by cyclic voltammetry as +1.73, +1.86, and +1.77 V (*vs.* NHE, for **AcCS^{3F}**, **AcCS^{5F}**, **AcCS^{6F}**, respectively); only 5-fluorination made antenna oxidation more difficult than in **AcCS** (E_{ox} = +1.81 V). PeT was calculated to be slightly less thermodynamically favoured in **EuL^{5F}**, and **EuL^{6F}** than in **EuL^{H}**, and more favoured in **EuL^{3F}** (ΔG(PeT) = −1.01, −1.14, −0.98, and −0.97 eV, for **EuL^{H}**, **EuL^{3F}**, **EuL^{5F}**, and **EuL^{6F}**, respectively (see ESI† for details)). Thus, the effects of fluorination on the antenna S_1, T_1 and E_{ox}, and in turn on ΔG(PeT) can be difficult to predict.

Table 2 Photophysical properties of **LnL^{F}** (Ln = Eu, Tb),[a] and τ_{rad}, Φ_{Ln}^{Ln}, and η_{sens} **EuL^{F}** [b]

	Φ_L[c,d] (%)	τ_{fl} (ns)	Φ_{Ln}[c] (%)	τ_{rad} (ms)	Φ_{Ln}^{Ln} (%)	η_{sens} (%)
TbL^{H}	5.1 (67%)	0.21(4)	22.5	—	—	—
TbL^{3F}	8.1 (63%)	0.39(2)	5.6	—	—	—
TbL^{5F}	4.6 (75%)	0.36(3)	21.7	—	—	—
TbL^{6F}	4.6 (78%)	0.25(4), 2.40(3)[e]	16.7	—	—	—
EuL^{H}	0.261 (3.4%)	—[f]	4.34	5.18[g], 4.73[h]	11.9[g], 13.1[h]	36.2[g]
EuL^{3F}	0.680 (5.3%)	0.93(6), 0.42(5)[e]	1.09	9.25[g], 5.10[h]	6.7[g], 12.3[h]	16.1[g]
EuL^{5F}	0.814 (13%)	0.47(6), 1.76(5)[e]	5.05	5.25[g], 5.11[h]	11.5[g], 11.8[h]	43.4[g]
EuL^{6F}	0.207 (3.5%)	0.20(1), 2.85(5)[e]	5.10	5.28[g], 5.19[h]	11.6[g], 11.8[h]	43.8[g]

[a] [**LnL**] = 10 μM in 10 mM PIPES buffered H_2O, pH 6.5. [b] Determined using the method in ref. 26. I_{tot}/I_{MD}: integral ratio of total Eu-centred corrected emission spectrum (570–800 nm) and $^5D_0 \rightarrow {}^7F_1$ band (582–603 nm), $A_{MD,0}$ = 14.65 s^{-1}, n = 1.333 (refractive index),[27] $\tau_{obs} = \tau_{H2O}$. [c] Relative to quinine sulfate (Φ = 0.59) in H_2SO_4 (0.05 M).[23] [d] In parentheses: compared to **GdL** analogue. [e] Biexponential fit better based on χ^2. [f] Too short to measure. [g] Calculated from the steady-state emission spectra. [h] Calculated from the time-resolved emission spectra.

The Ln(III) luminescence lifetimes (τ_{H2O}) were measured by time-resolved emission spectroscopy. The decays were monoexponential. τ_{H2O} values varied for Ln = Tb but were almost identical for all **EuL** ($\sim$0.61 ms) (Table S4, ESI†). The number of Ln(III)-bound water molecules (q) were q = 1 for **EuL**. Deviations for **TbL** from q = 1 could be due to BET, which makes this method inapplicable,[24,25] or the result of the typical error of q $\pm$0.5.

TbL^{5F} and **TbL^{H}** had the highest Tb-centred luminescence quantum yields (Φ_{Ln} = 21.7% and 22.5%, respectively, values identical within experimental error). The low Φ_{Ln} of **TbL^{3F}** is presumably the result of BET. **EuL^{5F}** and **EuL^{6F}** had Φ_{Ln} $\sim$5%, which is higher than most Eu(III) complexes with similar structures, *i.e.* uncharged do3a-based emitters with secondary amide-linked carbostyril antenna, including **EuL^{H}** (Φ_{Ln} = 4.34%). **EuL^{3F}**, however, had low Φ_{Ln} = 1.09%. Unlike **TbL^{3F}**, **EuL^{3F}** does not suffer from BET, therefore, an alternative explanation for the poor performance of this emitter was necessary.

Φ_{Ln} is the product of the intrinsic quantum yield of the Ln(III) (ϕ_{Ln}^{Ln}) and the Ln(III) sensitisation efficiency (η_{sens}, eqn (1)), *i.e.* the efficiency of Ln(III) excited state population. For Eu(III) ϕ_{Ln}^{Ln} can be determined from the corrected emission spectrum.[26]

$$\phi_{Ln} = \eta_{sens} \cdot \phi_{Ln}^{Ln} = \eta_{sens} \cdot \frac{\tau_{obs}}{\tau_{rad}} \quad (1)$$

In **EuL^{5F}** and **EuL^{6F}** η_{sens} is increased compared to **EuL^{H}**, presumably due to a combination of the small adjustments in spectral overlap and PeT quenching. **EuL^{3F}** had markedly lower η_{sens} and ϕ_{Ln}^{Ln} than the other **EuL** (Table 2). The steady-state and time-resolved **EuL^{3F}** emission spectra have different shapes. Eu(III) spectra are sensitive to coordination environment, and these differences indicate the presence of several emissive species.[21] The signal of the slow-decaying component dominating the time-resolved spectrum resembles the **EuL^{5F}**/**EuL^{6F}**/**EuL^{H}** spectra. Contribution from the fast-decaying species modifies the steady-state **EuL^{3F}** spectrum. If τ_{obs} is assumed unchanged, the steady-state spectral shape yields a lower overall ϕ_{Ln}^{Ln} (Table 2). The spectrum of **TbL^{3F}** is similarly time-dependent, but not those of **Eu/TbL^{5F}** and **Eu/TbL^{6F}**. The reasons for the diminished η_{sens} of **EuL^{3F}** are unclear. PeT is more favoured in **EuL^{3F}** than in **EuL^{5F}** and **EuL^{6F}**, and **EuL^{F}** have much lower Φ_{L} than the corresponding **GdL^{F}**, which is consistent with PeT quenching. The τ_{fl} of **EuL^{F}** and **GdL^{F}**, however, cannot be compared directly. The biexponential decay of the **EuL^{F}** antenna fluorescence suggested the presence of additional emitters to those seen in **GdL^{F}**. Further work is therefore needed to understand the effect of fluorination on EnT and PeT.

In conclusion, monofluorinated 7-aminocarbostyrils, obtained *via* a photochemical cyclisation, were competent sensitisers of Eu(III) and Tb(III) emission. The position of the fluorine had a dramatic impact on the antenna and Ln(III) photophysical properties, rendering the emission oxygen-sensitive (**TbL^{3F}**, **TbL^{4F}**), and increasing (**EuL^{5F}**, **EuL^{6F}**), or decreasing Φ_{Ln}, (**TbL^{3F}**, **TbL^{6F}**, **EuL^{3F}**) compared to non-fluorinated **LnL^{H}**. 5-Fluorination improved Eu(III) emission without negatively impacting Tb(III) luminescence. Remote fluorination influenced the excited-state behaviour of **LnL^{3F}**. Work towards the 4-fluorinated isomer, and ligands containing other EWGs than fluorine is ongoing.

D. K. did all experiments except the crystallographic analysis, which was done by A. O. K. E. B. designed the project, secured funding, and supervised the work. All authors contributed to data analysis and manuscript writing.

This work was funded by Knut och Alice Wallenbergs Stiftelse (Dnr: 2018.0066) and Vetenskapsrådet (2021-04625). We thank Eirini Servetas for help with the synthesis, and Salauat R: Kiraev for the critical reading of the manuscript.

Conflicts of interest

There are no conflicts to declare.

Notes and references

1 D. Parker, J. D. Fradgley and K.-L. Wong, *Chem. Soc. Rev.*, 2021, **50**, 8193–8213.
2 C. D.-S. Brites, S. Balabhadra and L. D. Carlos, *Adv. Opt. Mater.*, 2019, **7**, 1801239.
3 A. de Bettencourt-Dias, in *Luminescence of Lanthanide Ions in Coordination Compounds and Nanomaterials*, John Wiley & Sons Ltd, 2014, ch01, pp. 1–48.
4 D. Kovacs and K. E. Borbas, *Coord. Chem. Rev.*, 2018, **364**, 1–9.
5 D. Kovacs, X. Lu, L. S. Mészáros, M. Ott, J. Andres and K. E. Borbas, *J. Am. Chem. Soc.*, 2017, **139**, 5756–5767.
6 D. Kovacs, E. Mathieu, S. R. Kiraev, J. A.-L. Wells, E. Demeyere, A. Sipos and K. E. Borbas, *J. Am. Chem. Soc.*, 2020, **142**, 13190–13200.
7 A. J. Wilkinson, D. Maffeo, A. Beeby, C. E. Foster and J. A.-G. Williams, *Inorg. Chem.*, 2007, **46**, 9438–9449.
8 D. Parker, P. K. Senanayake and J. A.-G. Williams, *J. Chem. Soc., Perkin Trans. 2*, 1998, 2129–2139.
9 D. Kovacs, S. R. Kiraev, D. Phipps, A. Orthaber and K. E. Borbas, *Inorg. Chem.*, 2020, **59**, 106–117.
10 D. Kovacs, D. Phipps, A. Orthaber and K. E. Borbas, *Dalton Trans.*, 2018, **47**, 10702–10714.
11 P. B. Glover, A. P. Bassett, P. Nockemann, B. M. Kariuki, R. Van Deun and Z. Pikramenou, *Chem. – Eur. J.*, 2007, **13**, 6308–6320.
12 N. A. Meanwell, *J. Med. Chem.*, 2018, **61**, 5822–5880.
13 D. Janasik and T. Krawczyk, *Chem. – Eur. J.*, 2022, **28**, e202102556.
14 A. M. Kenwright, I. Kuprov, E. De Luca, D. Parker, S. U. Pandya, P. K. Senanayake and D. G. Smith, *Chem. Commun.*, 2008, 2514–2516.
15 J. Ruiz-Cabello, B. P. Barnett, P. A. Bottomley and J. W.-M. Bulte, *NMR Biomed.*, 2011, **24**, 114–129.
16 X. Deng, J. Rong, L. Wang, N. Vasdev, L. Zhang, L. Josephson and S. H. Liang, *Angew. Chem., Int. Ed.*, 2019, **58**, 2580–2605.
17 D. van der Born, A. Pees, A. J. Poot, R. V.-A. Orru, A. D. Windhorst and D. J. Vugts, *Chem. Soc. Rev.*, 2017, **46**, 4709–4773.
18 O. Bouazzaoui, K. Rousée, J. K. Mulengi, X. Pannecoucke, J.-P. Bouillon and S. Couve-Bonnaire, *Eur. J. Org. Chem.*, 2018, 3705–3715.
19 P. Ung, M. Clerc, H. Huang, K. Qiu, H. Chao, M. Seitz, B. Boyd, B. Graham and G. Gasser, *Inorg. Chem.*, 2017, **56**, 7960–7974.
20 G.-L. Law, R. Pal, L. O. Palsson, D. Parker and K.-L. Wong, *Chem. Commun.*, 2009, 7321–7323.
21 K. Binnemans, *Coord. Chem. Rev.*, 2015, **295**, 1–45.
22 S. Susumu and W. Masanobu, *Bull. Chem. Soc. Jpn.*, 1970, **43**, 1955–1962.
23 K. Suzuki, A. Kobayashi, S. Kaneko, K. Takehira, T. Yoshihara, H. Ishida, Y. Shiina, S. Oishi and S. Tobita, *Phys. Chem. Chem. Phys.*, 2009, **11**, 9850–9860.
24 A. Beeby, I. M. Clarkson, R. S. Dickins, S. Faulkner, D. Parker, L. Royle, S. A.-S. de, J. A.-G. Williams and M. Woods, *J. Chem. Soc., Perkin Trans. 2*, 1999, 493–504.
25 R. M. Supkowski and W. D. Horrocks Jr., *Inorg. Chim. Acta*, 2002, **340**, 44–48.
26 M. H.-V. Werts, R. T.-F. Jukes and J. W. Verhoeven, *Phys. Chem. Chem. Phys.*, 2002, **4**, 1542–1548.
27 A. H. Harvey, J. S. Gallagher and J. M.-H. L. Sengers, *J. Phys. Chem. Ref. Data*, 1998, **27**, 761–774.

